Cancer Research

Hypoxia Induces Escape from Innate Immunity in Cancer Cells via Increased Expression of ADAM10: Role of Nitric Oxide

Ivraym B. Barsoum[1], Thomas K. Hamilton[1], Xin Li[1], Tiziana Cotechini[1], Ellen A. Miles[1], D. Robert Siemens[1,2], and Charles H. Graham[1,2,3]

Abstract

One key to malignant progression is the acquired ability of tumor cells to escape immune-mediated lysis. Whereas tumor hypoxia is known to play a causal role in cancer metastasis and resistance to therapy, the link between hypoxia and immune escape in cancer remains poorly understood. Here, we show that hypoxia induces tumor cell resistance to lysis mediated by immune effectors and that this resistance to lysis occurs via a hypoxia-inducible factor-1 (HIF-1)–dependent pathway linked to increased expression of the metalloproteinase ADAM10. This enzyme is required for the hypoxia-induced shedding of MHC class I chain–related molecule A (MICA), a ligand that triggers the cytolytic action of immune effectors, from the surface of tumor cells. Indeed, our findings show a mechanistic link between hypoxia-induced accumulation of the α-subunit of HIF-1 (HIF-1α), increased expression of ADAM10, and decreased surface MICA levels leading to tumor cell resistance to lysis mediated by innate immune effectors. Nitric oxide mimetic agents interfered with the hypoxia-induced accumulation of HIF-1α and with the hypoxia-induced upregulation of ADAM10 expression required for decreased surface MICA expression and resistance to lysis. Furthermore, treatment of tumor-bearing mice with nitroglycerin, a nitric oxide mimetic, attenuated tumor growth by a mechanism that relied upon innate immune effector cells. Together, these findings reveal a novel mechanism by which the hypoxic tumor microenvironment contributes to immune escape in cancer, lending support to potential immunotherapeutic strategies involving the use of nitric oxide mimetics. *Cancer Res; 71(24); 7433–41. ©2011 AACR.*

Introduction

Studies conducted in the last 15 years have provided convincing evidence that the immune system plays a critical role in the prevention and control of cancer (1). However, an important aspect of malignant progression is the acquired ability of tumor cells to escape detection and destruction by the innate and adaptive arms of the immune system (1).

While many studies have shown the important contribution of tumor hypoxia to the acquisition of malignant properties in cancer cells, such as resistance to chemotherapeutic agents (2–4) and increased metastatic potential (5–7), the effect of hypoxia on tumor immune escape remains poorly understood. It has been reported that hypoxia stimulates in tumor cells the release of immunosuppressive molecules (8–10), and more recently, that it increases lung cancer cell resistance to cytotoxic T-cell–mediated lysis (11). Other studies have focused on assessing the direct effect of hypoxia on the activity of innate immune effectors rather than on hypoxia-induced adaptations of tumor cells that might endow them with resistance to immunosurveillance (12, 13). We previously showed that *in vitro* exposure of tumor cells to hypoxia increases their resistance to lysis mediated by interleukin (IL)-2–activated peripheral blood lymphocytes (IL-2/PBL) via a mechanism secondary to deficient endogenous nitric oxide signaling (14). This effect of hypoxia was due to the shedding of MHC class I chain–related molecule A (MICA) from the tumor cell surface.

Both MICA and its closely related MICB molecule play important roles in tumor surveillance by natural killer (NK) cells, lymphokine-activated killer (LAK) cells, and cytotoxic T cells (15). While MIC molecules are absent from most normal tissues, they are induced by cellular stresses, such as exposure to carcinogens and infection, and are expressed in various types of carcinomas and some hematopoietic malignancies (16). In humans, the interaction of cell surface MIC with the dominant activating natural killer group 2D (NKG2D) receptor complexes on NK, LAK, and effector T cells leads to the activation of innate and adaptive immune responses and the subsequent lysis of the tumor cells (17). Thus, MIC–NKG2D

Authors' Affiliations: Departments of [1]Anatomy and Cell Biology, [2]Urology, and [3]Pharmacology and Toxicology, Queen's University, Kingston, Ontario, Canada

Note: Supplementary data for this article are available at Cancer Research Online (http://cancerres.aacrjournals.org/).

I.B. Barsoum and T.K. Hamilton contributed equally to this study.

Corresponding Author: Charles H. Graham, Botterell Hall Room 859, Queen's University, Kingston, ON K7L 3N6, Canada. Phone: 613-533-2852; Fax: 613-533-2022; E-mail: graham@queensu.ca

doi: 10.1158/0008-5472.CAN-11-2104

interactions are critical to the surveillance function of immune effectors; consequently, decreased expression of MIC molecules on the surface of malignant cells represents an important aspect of immune escape.

Given that NKG2D ligands play such a critical role in immunosurveillance of cancer, it is important to elucidate mechanisms responsible for decreasing the levels of these molecules on the cell membrane and to determine the potential contribution of the tumor microenvironment to the regulation of these mechanisms. One important mechanism involves the proteolytic cleavage and release of the ectodomains of NKG2D ligands. Studies have revealed that transmembrane metalloproteinases including members of the ADAM (a disintegrin and metalloproteinase) enzymes, that is, ADAM9, ADAM10, and ADAM17, as well as matrix metalloproteinase 14 are responsible for the shedding of MICA and MICB from the surface of various cell types (18–20). Interestingly, these metalloproteinases have also been implicated in other aspects of malignant progression such as tumor growth, invasion, and metastasis.

Here, we provide evidence that hypoxia contributes to tumor cell resistance to lysis mediated by IL-2/PBLs through stimulation of ADAM10 expression and, consequently, decreased levels of MICA on the tumor cell membrane. We also show that this mechanism of immune escape is blocked by nitric oxide via inhibition of hypoxia-inducible factor-1α (HIF-1α) accumulation. The latter is the oxygen-regulated subunit of HIF-1, a transcription factor responsible for cellular adaptations to hypoxia (21).

Materials and Methods

Cells and culture conditions

Human DU145 prostate cancer and MDA-MB-231 breast cancer cells were obtained from the American Type Culture Collection. These cell lines were tested for mycoplasma contamination, but their identity had not been confirmed within the last 6 months prior to initiation of this study. Cells were maintained in RPMI-1640 medium supplemented with 10% FBS (Invitrogen Canada Inc.). For incubations in standard conditions (20% O_2), cells were placed in a Thermo CO_2 incubator. For incubations in hypoxia (0.5% O_2), cells were placed in a chamber that was flushed with a gas mixture of 5% CO_2/95% N_2. Oxygen concentrations within the chamber were maintained at 0.5% by means of a ProOx 110 oxygen regulator (Biospherix). Additional culture conditions included incubation of tumor cells with or without nitroglycerin (glyceryl trinitrate; GTN), diethylenetriamine-nitric oxide (DETA-NO), or 8-bromo-cGMP (8-Br-cGMP).

siRNA transfection

A transfection reagent, siPORT NeoFX (Ambion Inc.) was used according to the manufacturer's instructions to introduce siRNA into cells. Both HIF-1α and ADAM10 siRNAs were validated and were obtained from Applied Biosystems.

Western blotting

Following incubation under various conditions, cells were snap frozen in liquid nitrogen and then lysed and sonicated. Samples were resolved on 6% to 10% SDS-PAGE and transferred onto Immobilon-P membranes (Millipore Corporation). Membranes were blocked for 1 hour and then incubated with primary antibody in TBS/1% milk (reconstituted powder) overnight at 4ºC. Membranes were then washed and incubated for 1 hour at room temperature with secondary antibody in TBS/1% milk. Secondary antibodies were detected with enhanced chemiluminescence (Amersham Biosciences) and exposed to Kodak X-Omat Blue film.

Assessment of surface MICA

Surface expression of MICA was analyzed by flow cytometry. Briefly, cells were collected and incubated with monoclonal mouse anti-human MICA antibody (Santa Cruz Biotechnology) for 1 hour on ice. After washing, cells were incubated with a fluorescein isothiocyanate (FITC)–conjugated goat anti-mouse antibody for 1 hour and analyzed with a Beckman Coulter EPICS Altra HSS flow cytometer (Beckman-Coulter Canada).

Quantitative real-time PCR

Total RNA was isolated by a High Pure RNA Isolation Kit (Qiagen Inc.) according to the manufacturer's protocol. One microgram of total RNA was reverse-transcribed with Transcriptor Reverse Transcriptase (Roche) using a random hexamer (Cortec). Quantitative real-time PCR (qRT-PCR) was done with a LightCycler 480 Real-Time PCR System (Roche Diagnostics Corp.). Primers for ADAM10 cDNA amplification were: forward 5′CTTCACAGACCGAGATTTTGATG3′ and reverse 5′CACATATTCCTCCAGAGCTTCC3′. β-Actin mRNA served as internal control.

Isolation and purification of murine NK cells

Two female and one male Balb/c mice (4–6 weeks in age) were euthanized, and their spleens were excised and placed in separate Petri dishes containing ice-cold PBS. To extract splenocytes, spleens were placed on a fine wire mesh, rinsed with PBS, and crushed with the plunger of a 10-mL syringe. Cells were resuspended in 15 mL of PBS and centrifuged for 10 minutes at 400 × *g*. Cell pellets were resuspended in NK cell isolation buffer [2 mmol/L ETDA, 0.5% bovine serum albumin in PBS]. NK cell isolation was done by magnetic cell sorting with an autoMACS separator and a murine NK cell Isolation kit (Miltenyi Biotec) according to the manufacturer's instructions.

Cytotoxicity assay

The sensitivity of DU145 prostate tumor cells to cytolysis mediated by IL-2–activated human PBLs isolated from 2 healthy donors and isolated murine splenic NK cells was determined by a LIVE/DEAD cell viability/cytotoxicity assay (Invitrogen). Prior to the assay, tumor cells were transfected with either HIF-1α siRNA or ADAM10 siRNA or scrambled siRNA (Ambion) and allowed to recover for 24 hours. After further incubation in 20% O_2 or 0.5% O_2 for 24 hours, DU145 prostate tumor cells were incubated with IL-2–activated PBLs or murine NK cells in 96-well culture plates at different lymphocyte:tumor cell ratios (100:1, 50:1, 25:1, and 12.5:1) for

4 hours at 37°C, in the absence or presence of blocking polyclonal goat anti-MICA antibody (0.5 μg/mL; R&D Systems). Cocultures were then incubated with red fluorescent ethidium homodimer-1 for 30 minutes at 37°C. Fluorescence in plates was analyzed using a fluorescence multiwell plate reader (Varioskan 3001; ThermoFisher Scientific). Cell lysis was evaluated by calculating the percentage of dead cells in each sample at the completion of the assay. This was determined according to the manufacturer's instructions using the following formula: $([F(645)_{sample} - F(645)_{min}]/[F(645)_{max} - F(645)_{min}]) \times 100 = \%$ dead cells.

Confocal immunofluorescence

Expression of ADAM10 in human DU145 cells cultured under standard (20% O_2) or hypoxic (0.5% O_2) conditions was assessed by confocal immunofluorescence using a monoclonal anti-ADAM10 antibody (R&D Systems). Controls consisted of cells incubated with mouse IgG.

Tumor growth study

Six- to 8-week-old male athymic NIH Swiss nude (*nu*/*nu*) mice (Taconic) were inoculated subcutaneously in the left hind flank with 2×10^6 DU145 cells in 0.2 mL of growth factor–reduced Matrigel. When the tumors reached a volume of 100 mm^3, mice were randomly divided in 4 groups of 10 to 20 mice each as follows: (i) NK/LAK cell–deficient mice treated with square 0.25 cm^2 Minitran transdermal patches (3M Pharmaceuticals) delivering 1.8 μg of GTN per hour and placed on the back of the neck; (ii) NK/LAK cell–deficient mice treated with transdermal placebo patches (see later for details on NK/LAK cell depletion); (iii) NK/LAK cell–competent mice treated with GTN patches; and (iv) NK/LAK cell–competent mice treated with placebo patches. Transdermal patches were changed daily and were covered with a thin layer of New Skin Liquid Bandage (Medtech) to prevent mice from removing them during treatment. Tumor growth was measured every 2 days with digital calipers, and tumor volumes were determined according to the formula $(\text{length} \times \text{width})^2 \times 0.5$. Mice were sacrificed after approximately 62 days of treatment. Studies were conducted in accordance with the guidelines of the Canadian Council on Animal Care.

NK/LAK cell depletion

To deplete mouse NK/LAK cell populations, anti-asialo GM1 antibody (Wako Chemicals) was injected intraperitoneally (i.p.; 100 μL) every 5 days for the duration of the tumor growth experiment (approximately 62 days). Antibody injections were initiated concurrently with application of the transdermal patches. Before initiating the tumor growth study, the efficacy of the anti-asialo GM1 antibody at depleting NK cells was confirmed by flow cytometric determination of $CD3^-$/$CD122^+$/$DX5^+$ splenocytes (representing activated NK cells) in a separate group of 3 mice that received 3 injections of anti-asialo GM1 antibody 5 days apart. Results of that experiment revealed an 80% reduction in the numbers of activated NK cells in mice injected with rabbit polyclonal anti-asialo GM1 antibody versus mice injected with normal rabbit serum (Supplementary Fig. S1A). Furthermore, the presence of NK/LAK cells in excised tumors at the end of the experiment was determined by immunohistochemistry for perforin (NK/LAK/$CD8^+$ T-cell marker) using a rabbit polyclonal antibody (Torrey Pines Biolabs). Results of that study revealed the presence of perforin-positive cells only in tumors from mice injected with normal rabbit serum and not in mice injected with anti-asialo GM1 antibody (Supplementary Fig. S1B).

Statistical analysis

Values are expressed as means ± SEM. For statistical comparisons, one-way ANOVA followed by Bonferroni multiple comparison *post hoc* test was used. For the cytotoxicity assays, differences in killing were determined by ANOVA of the *y*-intercepts of the linear regressions of data from individual treatment groups. For the *in vivo* experiments, statistically significant differences in tumor growth were determined by comparing the slopes of the $\log_{10}$-transformed volumes of individual tumors using the exact Wilcoxon–Mann–Whitney test. Tumor growth curves were found to fit an exponential model. All statistical tests were 2-tailed. Sample sizes and number of times experiments were repeated are indicated in the figure legends. Number of asterisks in the figures indicates the level of statistical significance as follows: *, $P < 0.05$; **, $P < 0.01$; ***, $P < 0.001$.

Results

Hypoxia-mediated inhibition of surface MICA expression and increased tumor cell resistance to innate immune cytotoxicity requires HIF-1α expression

To determine whether the hypoxia-mediated inhibition of surface MICA expression is dependent on HIF-1 transcriptional activity, we knocked down HIF-1α using validated siRNA. Western blot analysis revealed that transient transfection of HIF-1α siRNA in DU145 prostate cancer cells effectively inhibited the hypoxic accumulation of HIF-1α protein (Supplementary Fig. S2). While transfection of DU145 prostate cancer cells and MDA-MB-231 breast cancer cells with control siRNA did not affect the expression of surface MICA as determined by flow cytometry, HIF-1α knockdown significantly attenuated the hypoxia-mediated decrease in surface MICA expression in these cells (Fig. 1A and B). Representative flow cytometric histograms are shown in Supplementary Fig. S3.

Results of cytotoxicity assays using cells transfected with control siRNA revealed that, compared with preincubation in 20% O_2, preincubation of DU145 prostate cancer cells in 0.5% O_2 resulted in increased resistance to IL-2/PBL–mediated cytolysis (Fig. 1C). In contrast, transfection with HIF-1α siRNA abrogated the hypoxia-induced resistance to IL-2/PBL–mediated cytolysis (Fig. 1D), indicating that HIF-1 is required for the hypoxia-induced resistance to innate immune cytotoxicity. To determine whether the decreased expression of surface MICA is causally linked to the hypoxia- and HIF-1–mediated resistance to cytolysis, we treated cells in the cytotoxicity assays with an anti-MICA antibody that blocks interactions of MICA with NKG2D. Results showed that anti-MICA antibody increased the resistance to cytolysis in control siRNA-transfected DU145 cells preincubated in 20% O_2 (Fig. 1C). However,

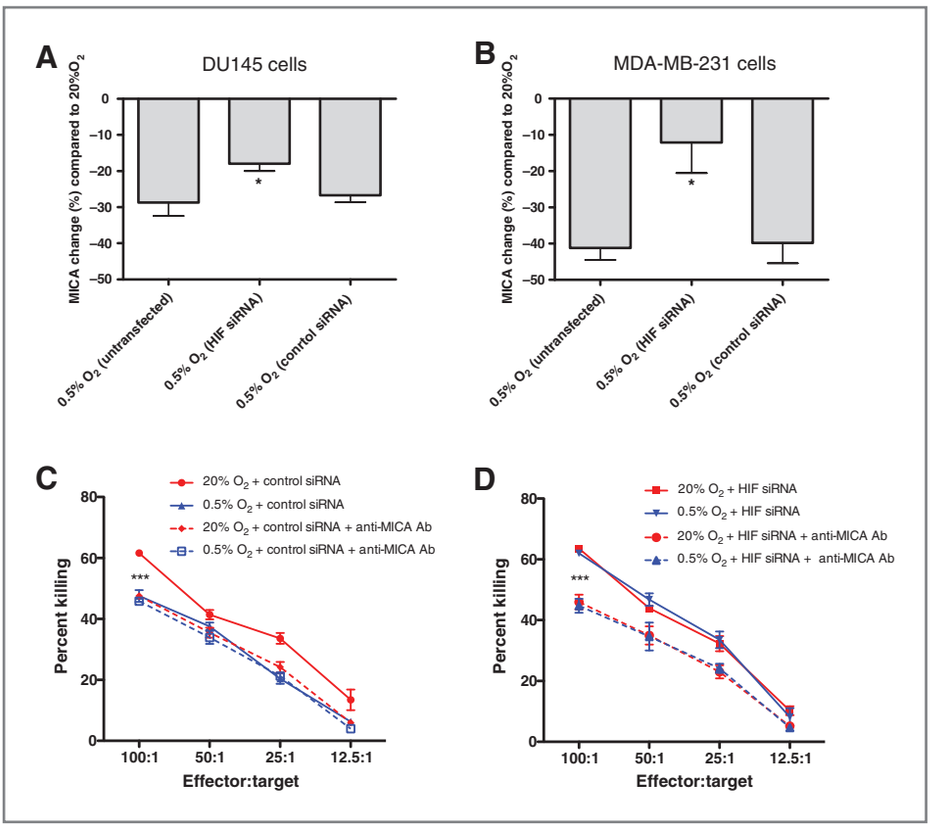

Figure 1. HIF-1α is required for decreased surface MICA expression and escape from innate immune-mediated lysis in tumor cells. A and B, flow cytometric analysis of surface MICA expression in DU145 (A) and MDA-MB-231 (B) cells either untransfected or transfected with control siRNA or HIF-1α siRNA. Asterisk in A and B indicates significant differences (*, $P < 0.05$, one-way ANOVA followed by Bonferroni multiple comparison *post hoc* test) versus the 2 other treatment groups. Data in A and B represent combined results of 6 to 9 independent flow cytometry experiments. C and D, cytolytic activity of human PBLs against DU145 cells preincubated in 20% O_2 or 0.5% O_2 following transient transfection with control siRNA (C) or HIF-1α siRNA (D). Percentage of killing was measured by a 2-color fluorescence cell viability assay. Data are presented as mean percentage of killing ±SEM and are representative of 2 to 4 independent experiments done in triplicate (i.e., experiments involving HIF-1α knockdown alone were done 4 times, whereas experiments involving HIF-1α knockdown ± MICA blocking antibody were done twice). Asterisks in C and D indicate significant differences (***, $P < 0.001$; ANOVA followed by Bonferroni multiple comparison *post hoc* test) in the *y*-intercepts of the linear regressions of the data represented by the curves above versus below the asterisks.

the anti-MICA antibody was unable to further increase the resistance to cytolysis in control siRNA-transfected DU145 cells preincubated in 0.5% O_2 (Fig. 1C), which already exhibited resistance even in the absence of anti-MICA antibody. Furthermore, anti-MICA antibody blocked the increased sensitivity to cytolysis in hypoxic DU145 cells transfected with HIF-1α siRNA (Fig. 1D). In fact, inclusion of anti-MICA antibody increased the resistance of DU145 cells to IL-2/PBL–mediated cytolysis to the same extent under all experimental conditions (Fig. 1C and D).

Hypoxia-mediated downregulation of surface MICA levels and resistance to cytolysis require ADAM10 expression

To determine whether ADAM10 and/or ADAM17 mediate the hypoxia-induced resistance to IL-2/PBL–mediated lysis of tumor cells, we first assessed whether hypoxia increases the expression of these enzymes. Results of Western blot analysis revealed that whereas hypoxia did not increase the levels of ADAM17 in DU145 or MDA-MB-231 cells (data not shown), the levels of ADAM10 in tumor cells increased following a 24-hour incubation in hypoxia (Fig. 2A and Supplementary Fig. S4). Confocal immunofluorescence provided further support for this observation (Fig. 2B), and results of qRT-PCR indicated that hypoxia increased the levels of ADAM10 transcript in DU145 and MDA-MB-231 (Fig. 2C and D) cells. While hypoxia increased the level of ADAM10 mRNA by approximately 8-fold, Western blot analysis revealed only a 2-fold increase in protein levels. This may be due to posttranscriptional regulatory mechanisms.

We also knocked down HIF-1α expression to assess whether HIF-1 is required for the hypoxia-induced upregulation of ADAM10 expression. Results of qRT-PCR showed that HIF-1α knockdown prevented the hypoxia-induced increase in ADAM10 transcript levels in DU145 and MDA-MB-231 cells (Fig. 2C and D), indicating that the hypoxia-induced expression of ADAM10 is HIF-1-dependent. In support of this conclusion, incubation of DU145 cells with cobalt chloride (100 μmol/L), a

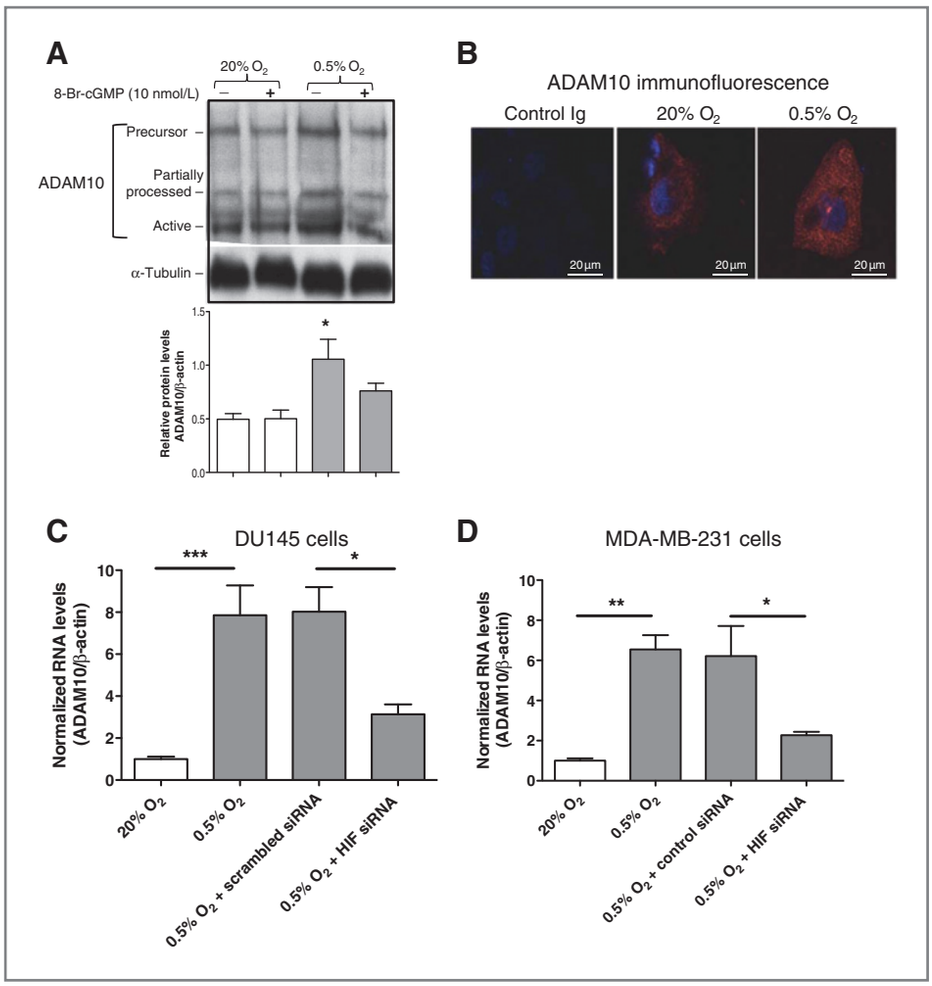

Figure 2. ADAM10 expression is induced by hypoxia via an HIF-1α–dependent mechanism. A, Western blot analysis of ADAM10 protein levels in DU145 cells cultured in 20% O_2 or 0.5% O_2 for 24 hours in the absence or presence of 8-Br-cGMP (10 nmol/L). Whereas hypoxia increased the levels of ADAM10 protein in DU145 cells, incubation with 8-Br-cGMP (10 nmol/L) during the exposure to hypoxia prevented the accumulation of ADAM10 protein. Results are representative of 3 experiments. Similarly, confocal immunofluorescence images of DU145 cells cultured in 20% O_2 or 0.5% O_2 and labeled with an anti-ADAM10 fluorescent antibody revealed increased fluorescence in cells incubated in hypoxia (B). Incubation of DU145 and MDA-MB-231 cells in 0.5% O_2 (vs. 20% O_2) for 24 hours resulted in significant increases in ADAM10 transcript levels as determined by qRT-PCR (C and D). This hypoxia-induced upregulation of ADAM10 mRNA expression was abrogated after HIF-1α knockdown (C and D). Bars indicate means ± SEM. *, $P < 0.05$; **, $P < 0.01$; ***, $P < 0.001$, one-way ANOVA followed by Bonferroni multiple comparison *post hoc* test. Results in C and D represent pooled data from 5 to 6 independent experiments.

known stabilizer of HIF-1α (22), resulted in increased ADAM10 mRNA levels (Supplementary Fig. S5).

To determine whether the hypoxia-mediated decrease in surface MICA levels and resistance of tumor cells to IL-2/PBL–mediated lysis is dependent on ADAM10, we knocked down ADAM10 expression using the siRNA approach. Western blot analysis and qRT-PCR revealed that introduction of ADAM10 siRNA in DU145 prostate cancer cells effectively inhibited the hypoxic accumulation of ADAM10 protein and mRNA (Supplementary Fig. S4). Knockdown of ADAM10 expression in DU145 cells abrogated the hypoxia-mediated decrease in surface MICA levels (Fig. 3A) as well as the hypoxia-induced resistance to IL-2/PBL–mediated cytolysis (Fig. 3B). Together, these findings indicate that hypoxia induces escape from immune effector–mediated cytolysis through an HIF-1–dependent mechanism requiring the upregulation of ADAM10. To further elucidate the link between increased expression of ADAM10, decreased surface MICA levels, and resistance to IL-2/PBL–mediated lysis, we conducted cytotoxicity assays in which MICA–NKG2D interactions were blocked with anti-MICA antibody. While ADAM10 knockdown restored the sensitivity of hypoxic DU145 cells up to levels similar to those observed in DU145 cells incubated in 20% O_2, anti-MICA antibody abrogated this effect (Fig. 3B). In fact, inclusion of anti-MICA antibody resulted in levels of resistance to cytolysis similar to those observed in hypoxia-exposed DU145 cells transfected with control siRNA (Fig. 3B). Together, these results are consistent with the concept that hypoxia acts in concert with ADAM10 to reduce the levels of surface MICA and to increase resistance to IL-2/PBL–mediated cytolysis.

Nitric oxide inhibits the hypoxia-induced expression of ADAM10 and the hypoxia-induced accumulation of HIF-1α

Nitric oxide in hypoxic tumor cells inhibits adaptations leading to malignant phenotypes such as increased metastatic ability and resistance to chemotherapeutic agents (6, 23, 24). Therefore, we examined whether nitric oxide signaling also regulates the hypoxia-induced upregulation of ADAM10 expression. Our results revealed that, indeed, activation of nitric oxide signaling with nitroglycerin (1 μmol/L) or DETA-NO (1 μmol/L) effectively attenuated the hypoxia-induced increases in ADAM10 transcript levels in DU145 prostate cancer cells and MDA-MB-231 breast cancer cells (Fig. 4A–C). Consistent with these results, 8-Br-cGMP (a downstream activator of nitric oxide signaling) inhibited the

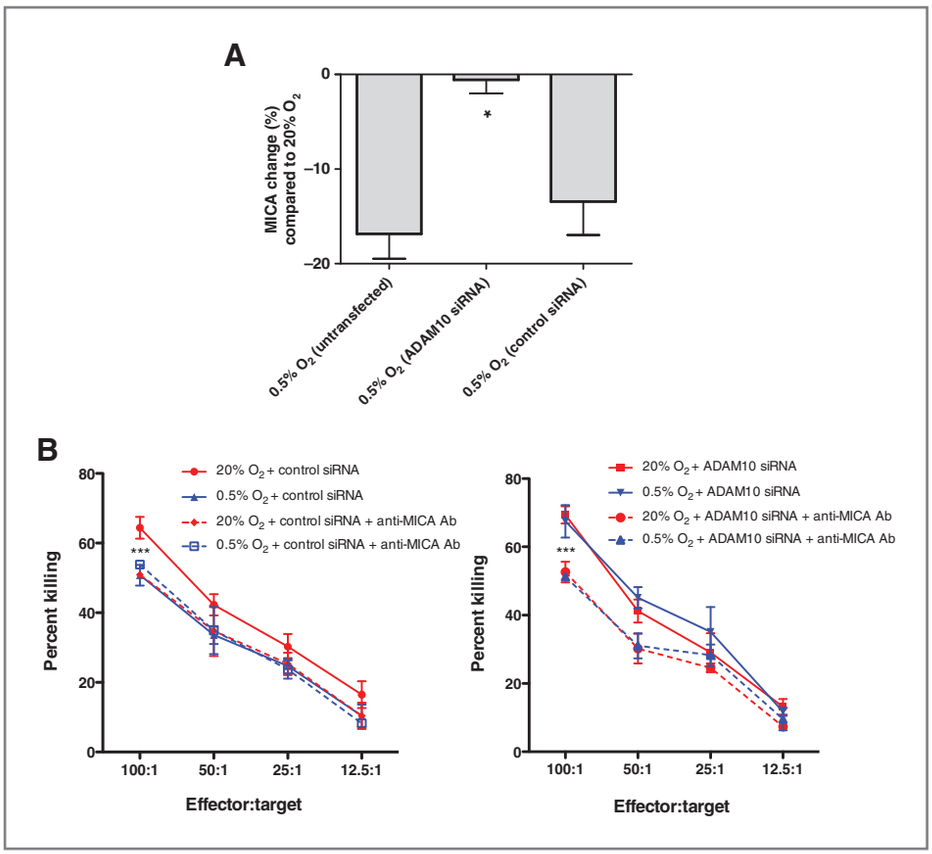

Figure 3. ADAM10 expression is required for decreased surface MICA expression and hypoxia-induced resistance to PBL-mediated lysis. A, flow cytometric analysis of surface MICA in DU145 cells cultured in 20% O_2 or 0.5% O_2 for 24 hours after transient transfection of control siRNA or ADAM10 siRNA revealed that ADAM10 expression is required for the hypoxia-mediated inhibition of surface MICA expression. Bars indicate means ± SEM. *, $P < 0.05$ (3 independent experiments). B, cytolytic activity of human PBLs against DU145 cells preincubated in 20% O_2 or 0.5% O_2 following transient transfection with scrambled siRNA or ADAM10 siRNA in the absence or presence of blocking anti-MICA antibody. Percentage of killing was measured by a 2-color fluorescence cell viability assay. Data shown are representative of results obtained from 2 to 4 independent experiments done in triplicate (i.e., experiments involving ADAM10 knockdown alone were done 4 times, whereas experiments involving ADAM10 knockdown ± MICA blocking antibody were done twice). Asterisks in B indicate significant differences (***, $P < 0.001$; ANOVA followed by Bonferroni multiple comparison *post hoc* test) in the *y*-intercepts of the linear regressions of the data represented by the curves above versus below the asterisks.

hypoxia-mediated increase in ADAM10 protein levels (Fig. 2A). Moreover, and in agreement with our previous findings (14), nitroglycerin at a concentration of 10 nmol/L significantly attenuated the hypoxia-induced release of MICA in the culture medium of DU145 cells as determined by a commercially available ELISA (Supplementary Fig. S6).

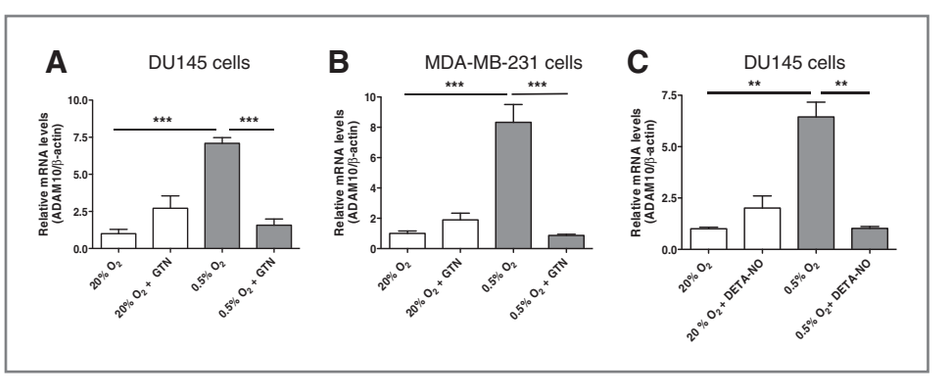

Figure 4. Nitric oxide mimetics prevent the hypoxia-induced upregulation of ADAM10 expression. qRT-PCR analysis of ADAM10 transcript levels in DU145 and MDA-MB-231 cells cultured in 20% O_2 or 0.5% O_2 with or without nitroglycerin (GTN; 1 μmol/L; A and B) or in DU145 cells incubated in 20% or 0.5% O_2 with or without DETA-NO (1 μmol/L; C). Results represent pooled data from 3 to 6 independent experiments. Bars represent mean ± SEM. **, $P < 0.01$; ***, $P < 0.001$, one-way ANOVA followed by Bonferroni multiple comparison *post hoc* test.

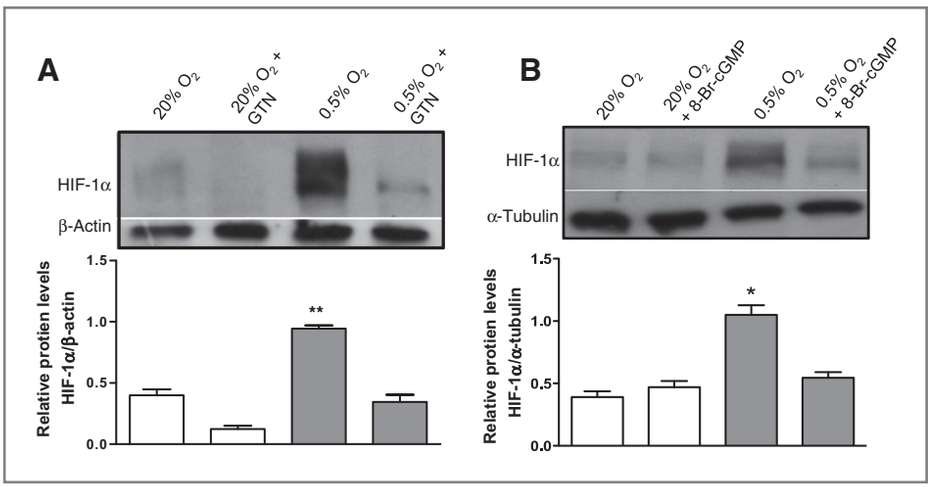

Figure 5. Nitric oxide mimetics prevent the hypoxia-induced upregulation of HIF-1α accumulation. Western blot analysis of endogenous HIF-1α protein levels in DU145 cells cultured in either 20% O_2 or 0.5% O_2 with or without 1 μmol/L nitroglycerin (A) or 10 nmol/L 8-Br-cGMP (B). Bars represent mean ± SEM. *, $P < 0.05$; **, $P < 0.01$, one-way ANOVA followed by Bonferroni multiple comparison *post hoc* test. Results represent pooled data from 3 to 4 independent experiments.

Previous studies showed that nitric oxide can interfere with the accumulation of HIF-1α under hypoxia (25, 26). On the basis of the observation that the hypoxia-induced increase of ADAM10 expression in tumor cells is HIF-1–dependent, we determined the effect of nitric oxide mimetic agents on HIF-1α accumulation. Western blot analysis revealed that nitroglycerin (1 μmol/L) and 8-Br-cGMP (10 nmol/L) were able to block the accumulation of HIF-1α in DU145 cells incubated in hypoxia (Fig. 5A and B). These results indicate that a mechanism by which nitric oxide mimetics interfere with the hypoxia-induced upregulation of ADAM10 expression is via inhibition of HIF-1α accumulation. They also provide evidence in support for a mechanism of inhibition of HIF-1α via the classical cGMP-dependent signaling pathway.

The nitric oxide mimetic nitroglycerin attenuates the growth of human prostate tumors in nude mice via a mechanism dependent on innate immune effector cells

On the basis of our present *in vitro* findings, we hypothesized that innate immune effector cells, such as NK cells and LAK cells, are responsible for the attenuation of tumor growth in nitroglycerin-treated mice. To test this hypothesis, we adopted a model in which human DU145 cells were injected subcutaneously into male NIH Swiss nude mice (T- and B-cell–deficient, NK/LAK cell–competent). While mouse tissues do not express MICA, these molecules, present on transplanted human tumor cells, can bind murine NKG2D and act as potent activating ligands (27). Indeed, results of cytotoxicity assays revealed that IL-2–activated mouse NK cells are capable of killing DU145 cells in a MICA-dependent manner, as inclusion of anti-MICA antibody decreased the sensitivity of tumor cells preincubated in 20% O_2 down to levels similar to those observed in DU145 cells preincubated in hypoxia (Supplementary Fig. S7). These results are in agreement with our results shown in Figs. 1 and 2 using IL-2–activated human PBLs.

DU145 prostatic tumors became palpable approximately 2 weeks following subcutaneous transplantation into nude mice and were allowed to grow for approximately 60 days. At the end of the study, tumors were excised, and HIF-1α and ADAM10 were localized in sections using immunofluorescence (Supplementary Fig. S8; method included in the legend). Results revealed that regions labeled with HIF-1α always overlapped with ADAM10 labeling. However, regions showing labeling for ADAM10 did not always exhibit HIF-1α immunoreactivity.

We observed that the subcutaneous growth of human DU145 prostate tumors in NIH Swiss nude mice was significantly attenuated after continuous administration of nitroglycerin (1.8 μg/h) via a transdermal patch (Fig. 6). However, this inhibition of tumor growth mediated by nitroglycerin was lost in mice depleted of their NK/LAK cells (see the Material and Methods section for details on immune effector cell depletion). These findings provide evidence in support of the concept that nitroglycerin attenuates *in vivo* tumor growth by sensitizing tumor cells to recognition and elimination by the innate immune system.

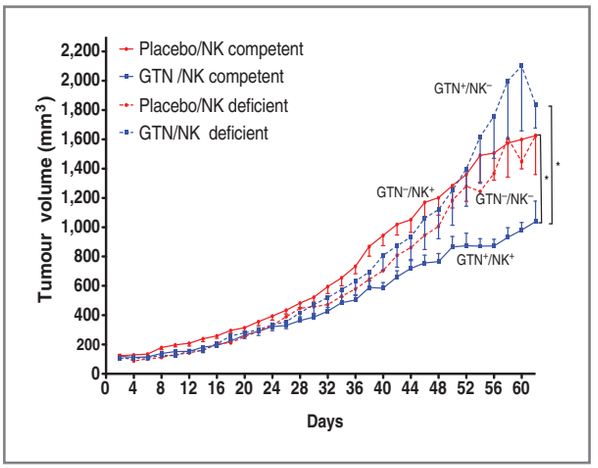

Figure 6. Effect of nitroglycerin and NK/LAK cell depletion on the growth of DU145 tumors transplanted into male NIH Swiss nude mice. Mean tumor volume per treatment group from start of treatment until sacrifice. Tumor growth curves were analyzed by comparing the slopes of the linear curves of the $\log_{10}$-transformed volumes across all measurements. Each treatment group consisted of 10 to 20 mice. Statistical differences between the slopes of the $\log_{10}$-transformed volumes were determined using the exact Wilcoxon–Mann–Whitney test. Results indicate that tumor growth was attenuated only in the group of NK/LAK cell–competent mice treated with nitroglycerin patches. *, $P < 0.05$.

Discussion

For malignant progression to occur in immunocompetent individuals, tumors must develop strategies to evade immunosurveillance. Some of these strategies include, among many, the release of immunosuppressive molecules (e.g., TGF-β, IL-10, and prostaglandins), escape from immune-mediated apoptosis, and the release of tumor cell surface antigens. Wu and colleagues reported the shedding of MIC molecules in advanced prostate cancers and that this shedding may be part of a mechanism of escape from immune cytotoxicity (28). Furthermore, a significant correlation between circulating soluble MICA levels and tumor stage and metastasis in patients with various malignancies has been reported (29).

In the present study, we showed that hypoxia, a well-recognized driver of malignant progression, contributes to immune escape in prostate and breast tumor cells by increasing the expression of ADAM10 in an HIF-1–dependent manner. We provide evidence that decreased MICA levels on the surface of tumor cells underlies the mechanism of immune escape induced by HIF-1 and ADAM10. Our results also reveal that activation of nitric oxide signaling interferes with this mechanism of immune escape.

Our study focused on the effect of hypoxia on tumor cell escape from innate immunity. To determine the effect of nitroglycerin on *in vivo* tumor cell susceptibility to lysis by innate immune effectors, we adopted an immunocompromised mouse tumor xenotransplantation model. NIH Swiss nude mice are deficient in B and T lymphocytes but have a full complement of NK cells and LAK cells. Our results showed that nonprimed IL-2–activated murine NK cells are capable of killing human DU145 cells via a MICA-dependent mechanism. Thus, nude mice are suitable for studies on tumor cell escape from innate immunity. Also, because antibody-mediated depletion of NK and LAK cells can be easily achieved in these mice, the effect of nitroglycerin on tumor growth can be assessed in the absence of cells from the adaptive arm of the immune system, such as T and B lymphocytes. Interestingly, in our study, nitroglycerin therapy failed to attenuate tumor growth in nude mice treated with anti-asialo GM1 antibody, indicating that innate immune effector cells, in this model, mediate the tumor growth-inhibitory effects of nitroglycerin.

Our previous studies revealed that activation of nitric oxide signaling inhibits the hypoxia-mediated acquisition of tumor cell invasiveness, metastatic potential, and resistance to chemotherapeutic agents (6, 23, 24). The results of the present study indicate that another important aspect of malignant progression, that is, escape from immunosurveillance is regulated in a similar manner. On the basis of our *in vitro* findings, it is likely that nitric oxide mimetics attenuate *in vivo* tumor growth by inhibiting HIF-1α accumulation in the tumor cells, thereby preventing ADAM10 expression and the subsequent shedding of MICA.

Interestingly, 2 different classes of nitric oxide mimetics, nitroglycerin and DETA-NO, were able to block the effect of hypoxia at the level of HIF-1α accumulation or ADAM10 expression. It was previously shown that certain nitric oxide mimetics that inhibit mitochondrial respiration under mildly hypoxic conditions, including DETA-NO, block HIF-1α accumulation as a result of a redistribution of intracellular oxygen leading to degradation of HIF-1α (25). However, in our study 8-Br-cGMP, an analogue of the nitric oxide signaling second messenger cGMP that does not inhibit mitochondrial function, also prevented HIF-1α accumulation. These results support the concept that NO-mediated inhibition of HIF-1α can occur via the classical cGMP-dependent signaling pathway.

In summary, our results show a novel mechanism by which hypoxia contributes to immune escape in tumor cells and provide evidence that activation of nitric oxide signaling interferes with this mechanism. The findings described here are important because they indicate that nitric oxide mimetics could potentially be used as immunosensitisers in the treatment and/or prevention of cancer.

Disclosure of Potential Conflicts of Interest

C.H. Graham and D.R. Siemens have ownership interest in Nometics Inc. and are consultant/advisory board members of Nometics Inc. No potential conflicts of interest were disclosed by the other authors.

Authors' Contributions

I.B. Barsoum and T.K. Hamilton did most of the experiments and data analysis. X. Li, T. Cotechini, and E.A. Miles conducted additional experimentation, including flow cytometric analysis of surface MICA, perforin immunohistochemistry, and ADAM10 immunofluorescence. D.R. Siemens and C.H. Graham developed the concepts and contributed to data interpretation. C.H. Graham wrote most of the manuscript and supervised the project.

Acknowledgments

The authors thank Matt Simpson for his assistance with the flow cytometric analysis, Jalna Meens for her help with the fluorescence microscopy, Andrew Day for his assistance with the statistical analysis of the tumor growth curves, Angie Black and Sylvia Robb for collecting human blood, Shannyn Macdonald-Goodfellow for general technical assistance, and Dr. Chandrakant Tayade for providing comments on the manuscript. I.B. Barsoum and T.K. Hamilton were recipients of a post-doctoral fellowship and a graduate studentship, respectively, from the Terry Fox Foundation Training Program in Transdisciplinary Cancer Research in Partnership with CIHR.

Grant Support

Financial support was provided by the Canadian Institutes of Health Research.

The costs of publication of this article were defrayed in part by the payment of page charges. This article must therefore be hereby marked *advertisement* in accordance with 18 U.S.C. Section 1734 solely to indicate this fact.

Received June 22, 2011; revised September 30, 2011; accepted October 11, 2011; published OnlineFirst October 17, 2011.

References

1. Schreiber RD, Old LJ, Smyth MJ. Cancer immunoediting: integrating immunity's roles in cancer suppression and promotion. Science 2011;331:1565–70.

2. Kalra R, Jones AM, Kirk J, Adams GE, Stratford IJ. The effect of hypoxia on acquired drug resistance and response to epidermal growth factor in Chinese hamster lung fibroblasts and

human breast-cancer cells *in vitro*. Int J Cancer 1993;54: 650–5.
3. Teicher BA. Hypoxia and drug resistance. Cancer Metastasis Rev 1994;13:139–68.
4. Sanna K, Rofstad EK. Hypoxia-induced resistance to doxorubicin and methotrexate in human melanoma cell lines *in vitro*. Int J Cancer 1994;58:258–62.
5. Sullivan R, Graham CH. Hypoxia-driven selection of the metastatic phenotype. Cancer Metastasis Rev 2007;26:319–31.
6. Postovit LM, Adams MA, Lash GE, Heaton JP, Graham CH. Nitric oxide-mediated regulation of hypoxia-induced B16F10 melanoma metastasis. Int J Cancer 2004;108:47–53.
7. Cuvier C, Jang A, Hill RP. Exposure to hypoxia, glucose starvation and acidosis: effect on invasive capacity of murine tumor cells and correlation with cathepsin (L + B) secretion. Clin Exp Metastasis 1997;15: 19–25.
8. Blay J, White TD, Hoskin DW. The extracellular fluid of solid carcinomas contains immunosuppressive concentrations of adenosine. Cancer Res 1997;57:2602–5.
9. Butler JJ, Mader JS, Watson CL, Zhang H, Blay J, Hoskin DW. Adenosine inhibits activation-induced T cell expression of CD2 and CD28 co-stimulatory molecules: role of interleukin-2 and cyclic AMP signaling pathways. J Cell Biochem 2003;89:975–91.
10. Wei J, Wu A, Kong LY, Wang Y, Fuller G, Fokt I, et al. Hypoxia potentiates glioma-mediated immunosuppression. PLoS One 2011;6:e16195.
11. Noman MZ, Buart S, Van Pelt J, Richon C, Hasmim M, Leleu N, et al. The cooperative induction of hypoxia-inducible factor-1 alpha and STAT3 during hypoxia induced an impairment of tumor susceptibility to CTL-mediated cell lysis. J Immunol 2009;182:3510–21.
12. Loeffler DA, Juneau PL, Heppner GH. Natural killer-cell activity under conditions reflective of tumor micro-environment. Int J Cancer 1991;48:895–9.
13. Fink T, Ebbesen P, Koppelhus U, Zachar V. Natural killer cell-mediated basal and interferon-enhanced cytotoxicity against liver cancer cells is significantly impaired under *in vivo* oxygen conditions. Scand J Immunol 2003;58:607–12.
14. Siemens DR, Hu N, Sheikhi AK, Chung E, Frederiksen LJ, Pross H, et al. Hypoxia increases tumor cell shedding of MHC class I chain-related molecule: role of nitric oxide. Cancer Res 2008;68:4746–53.
15. Doubrovina ES, Doubrovin MM, Vider E, Sisson RB, O'Reilly RJ, Dupont B, et al. Evasion from NK cell immunity by MHC class I chain-related molecules expressing colon adenocarcinoma. J Immunol 2003;171:6891–9.
16. González S, Groh V, Spies T. Immunobiology of human NKG2D and its ligands. Curr Top Microbiol Immunol 2006;298:121–38.
17. Groh V, Wu J, Yee C, Spies T. Tumour-derived soluble MIC ligands impair expression of NKG2D and T-cell activation. Nature 2002;419: 734–8.
18. Waldhauer I, Goehlsdorf D, Gieseke F, Weinschenk T, Wittenbrink M, Ludwig A, et al. Tumor-associated MICA is shed by ADAM proteases. Cancer Res 2008;68:6368–76.
19. Liu G, Atteridge CL, Wang X, Lundgren AD, Wu JD. The membrane type matrix metalloproteinase MMP14 mediates constitutive shedding of MHC class I chain-related molecule A independent of A disintegrin and metalloproteinases. J Immunol 2010;184:3346–50.
20. Kohga K, Takehara T, Tatsumi T, Ishida H, Miyagi T, Hosui A, et al. Sorafenib inhibits the shedding of major histocompatibility complex class I-related chain A on hepatocellular carcinoma cells by down-regulating a disintegrin and metalloproteinase 9. Hepatology 2010;51: 1264–73.
21. Wang GL, Jiang BH, Rue EA, Semenza GL. Hypoxia-inducible factor 1 is a basic-helix-loop-helix-PAS heterodimer regulated by cellular O2 tension. Proc Natl Acad Sci U S A 1995;92:5510–4.
22. Semenza GL. Hypoxia-inducible factor 1 (HIF-1) pathway. Sci STKE 2007;2007:cm8.
23. Matthews NE, Adams MA, Maxwell LR, Gofton TE, Graham CH. Nitric oxide-mediated regulation of chemosensitivity in cancer cells. J Natl Cancer Inst 2001;93:1879–85.
24. Frederiksen LJ, Sullivan R, Maxwell LR, Macdonald-Goodfellow SK, Adams MA, Bennett BM, et al. Chemosensitization of cancer *in vitro* and *in vivo* by nitric oxide signaling. Clin Cancer Res 2007;13:2199–206.
25. Hagen T, Taylor CT, Lam F, Moncada S. Redistribution of intracellular oxygen in hypoxia by nitric oxide: effect on HIF1alpha. Science 2003;302:1975–8.
26. Sogawa K, Numayama-Tsuruta K, Ema M, Abe M, Abe H, Fujii-Kuriyama Y. Inhibition of hypoxia-inducible factor 1 activity by nitric oxide donors in hypoxia. Proc Natl Acad Sci U S A 1998;95:7368–73.
27. Wiemann K, Mittrucker HW, Feger U, Welte SA, Yokoyama WM, Spies T, et al. Systemic NKG2D down-regulation impairs NK and CD8 T cell responses *in vivo*. J Immunol 2005;175:720–9.
28. Wu JD, Higgins LM, Steinle A, Cosman D, Haugk K, Plymate SR. Prevalent expression of the immunostimulatory MHC class I chain-related molecule is counteracted by shedding in prostate cancer. J Clin Invest 2004;114:560–8.
29. Holdenrieder S, Stieber P, Peterfi A, Nagel D, Steinle A, Salih HR. Soluble MICA in malignant diseases. Int J Cancer 2006;118:684–7.